Physical Carrier Sensing and Spatial Reuse in Multirate and Multihop Wireless Ad Hoc Networks

Hongqiang Zhai and Yuguang Fang
Department of Electrical & Computer Engineering
University of Florida, Gainesville, Florida 32611-6130
Tel: (352) 846-3043, Fax: (352) 392-0044
E-mail: zhai@ecel.ufl.edu and fang@ece.ufl.edu

Abstract— **Physical carrier sensing is an effective mechanism of medium access control (MAC) protocols to reduce collisions in wireless networks, and the size of the carrier sensing range has a great impact on the system performance. Previous studies have shown that the MAC layer overhead plays an important role in determining the optimal carrier sensing range. However, variable transmission ranges and receiver sensitivities for different channel rates and the impact of multihop forwarding have been ignored. In this paper, we investigate the impacts of these factors as well as several other important factors, such as SINR (signal to interference plus noise ratio), node topology, hidden/exposed terminal problems and bidirectional handshakes, on determining the optimum carrier sensing range to maximize the throughput through both analysis and simulations. The results show that if any one of these factors is not addressed properly, the system performance may suffer a significant degradation. Furthermore, considering both multirate capability and carrier sensing ranges, we propose to use bandwidth distance product as a routing metric, which improves end-to-end throughput by up to 27% in the simulated scenario.**

I. Introduction

Wireless ad hoc networks have wide applications in many situations wherever wireless communication and networking are preferred for convenience and/or low cost, such as wireless mesh networks and sensor networks. In such networks, medium access control (MAC) protocol plays a key role to coordinate the users' access to the shared medium. The IEEE 802.11 [1] protocol is a kind of CSMA/CA (carrier sense multiple access with collision avoidance) MAC protocols and it has been the standard of the wireless LANs. The 802.11 DCF (distributed coordination function) protocol has been also widely studied in the wireless multihop ad hoc networks due to its simple implementation and distributed nature.

Carrier sensing is a fundamental mechanism in CSMA/CA protocols. Each user senses the channel before a transmission and defers the transmission if it senses a busy channel to reduce the collision. This mechanism consists of physical carrier sensing and virtual carrier sensing. In the physical carrier sensing, the channel is determined busy if the sensed signal power is larger than a carrier sensing threshold CS_{th} or idle otherwise. In the virtual carrier sensing, each user regards the channel busy during the period indicated in the MAC header of the MAC frames, such as RTS (ready to send), CTS (clear to send), DATA, and ACK (acknowledgement) defined in the IEEE 802.11 protocol.

The virtual carrier sensing mechanism can only notify the nodes in the transmission range of the occupied medium, in which a transmission can be decoded correctly if the interference level is small enough. Transmissions outside of this range can introduce enough interference to corrupt the reception in many cases. In addition, some ongoing transmissions may not be decoded correctly due to other transmissions nearby, resulting in the failure of the virtual carrier sensing. Hence virtual carrier sensing cannot rule out collisions from inside of the transmission range and is incapable of avoiding collisions from outside of the transmission range.

Physical carrier sensing range, in which a transmission is heard but may not be decoded correctly, can be much larger than the transmission range and hence it can be more effective than the virtual carrier sensing in avoiding the interference especially in the multihop networks. However, large carrier sensing range reduces spatial reuse and affects the aggregate throughput because any potential transmitters, which sense a busy channel, are required to keep silent. Therefore, the optimum carrier sensing range should balance the spatial reuse and the impact of collisions in order to optimize the system performance.

The IEEE 802.11 a/b/g protocols provide multiple channel rates in wireless multihop ad hoc networks. Different channel rates have different transmission ranges, requirements of SINR (signal to interference plus noise ratio) and receiver sensitivity. Does each rate require a different optimum carrier sensing threshold? How can we set the carrier sensing threshold when multiple rates coexist? Furthermore, multiple forwardings are common for multihop flows and may force a significant change of the optimum carrier sensing threshold from the case when only one-hop flows are considered. Higher channel rates result in shorter transmission delay but also have shorter ranges. We must be careful to select the appropriate channel rate to maximize the system performance in terms of end-to-end delay/throughput and power consumption, which are all important performance metrics for multihop flows. To optimize

This work was supported in part by the U.S. Office of Naval Research under Young Investigator Award N000140210464 and by the National Science Foundation under Faculty Early Career Development Award ANI-0093241 and under grant DBI-0529012.

This full text paper was peer reviewed at the direction of IEEE Communications Society subject matter experts for publication in the Proceedings IEEE Infocom.

the end-to-end performance of multihop flows, carrier sensing range and spatial reuse as well as hop distance must be appropriately addressed.

The default setting of the physical carrier sensing threshold and the carrier sensing strategy in the widely used network simulation tools ns2 and OPNET are not optimum in most cases. The excessive collisions result in false link/route failures followed by rerouting and unnecessary end-to-end retransmissions of TCP packets. Poor performance at the MAC layer as well as at the higher layers has been reported in many literatures especially for multihop flows in wireless ad hoc networks ([2]–[6]). Furthermore, these simulation tools have not considered the variable requirements of carrier sensing ranges and transmission ranges when multiple channel rates of the IEEE 802.11 protocols are used, hence the simulation studies may not reflect the performance of real products.

Many papers have already noticed the impact of carrier sensing and spatial reuse on the system performance. Xu et al. [7] indicate that virtual carrier sensing via RTS/CTS is far from enough to solve the interference and larger physical carrier sensing range can help in some degree. In [8]–[10], co-channel interference is analyzed to derive the spatial reuse and the capacity of wireless networks wherein a minimum SINR is necessary for successful communication. Gobriel et al. [11] construct a collision model together with an interference model of a uniformly distributed network to derive the optimum transmission power that yields maximum throughput and minimum energy consumption per message. Li et al. [12] identify several unfairness problems due to the EIFS duration required by the carrier sensing mechanism and propose to use variable EIFS duration.

Recently, several work have also attempted to identify the optimum carrier sensing range. Deng et al. [13] illustrate the impact of physical carrier sensing range on the aggregate throughput of one-hop flows and propose a reward formulation to characterize the trade-off between the spatial reuse and packet collisions. Zhu et al. [14] have attempted to identify the optimal carrier sensing threshold that maximizes the spatial reuse for a regular topology. Yang and Vaidya [15] show that MAC layer overheads have a great impact on the choice of carrier sensing range. However, the interactions between carrier sensing range and variable transmission ranges for different channel rates, as well as their impact on the network performance, have not been identified by prior research, and the impact of multihop forwarding on the carrier sensing range have not been addressed either. There are also several other important factors needed to be further studied to determine an optimum carrier sensing range, such as variable requirements of SINR and receiver sensitivities for different channel rates, bidirectional handshakes, tradeoff between spatial reuse and collisions, node density and network topology, and the impact on higher layers' performance. In this paper, we use both analyses and simulations to illustrate the relationships between all these factors and the system performance. We demonstrate that if any of these factors is not considered properly in determining the optimal carrier sensing range, the system performance can suffer a significant loss.

The rest of this paper is organized as follows. Section II studies the optimum carrier sensing range subject to various factors and its impact on the aggregate one-hop throughput. Based on the results in Section II, we illustrate in Section III how to set the carrier sensing threshold in a multirate ad hoc network and how it affects the end-to-end throughput, delay and energy consumption of multihop flows. In Section IV, we introduce several important ns2 extensions and conduct simulation studies to verify the analytical results. Finally, Section V concludes this paper.

II. Optimum Carrier Sensing Range

In this section, we first derive the optimum carrier sensing range at the worst case scenario where there exists the most severe interference. Both the Shanon capacity and the 802.11's discrete channel rates are considered in the analytical studies. Then we discuss the tradeoff between the hidden terminal problem and the exposed terminal problem in maximizing the aggregate throughput and the impact of random topology and bidirectional handshakes.

A. Aggregate Throughput and SINR at the Worst Case

We first introduce several notations before we discuss the optimum carrier sensing range. RX_{th} denotes the smallest power level of the received signal required for correctly decoding at the receiver. It determines the transmission range and the corresponding maximum transmission distance d_t. CS_{th} denotes the carrier sensing threshold, and a node senses an idle channel if the sensed power level is less than CS_{th} or a busy channel otherwise. It determines the maximum sensing distance d_c. X represents the relative size of the carrier sensing range compared to the transmission range and

$$X = \frac{d_c}{d_t} \tag{1}$$

It can be shown that the maximum interference level is achieved when six other nodes are transmitting simultaneously at the boundary of the carrier sensing range of each transmitter as shown in Fig. 1 given that any two transmitters must be d_c away from each other. Similar to the cellular networks scenario, these 6 nodes are the first tier interference nodes. Since any other interference nodes are far away and contribute much smaller interference than the first tier interference nodes, we ignore them when calculating the SINR. To facilitate the calculation, we also show the two-dimensional coordinates of the nodes in Fig. 1(b), where α denotes the included angle between N_0D_0 and N_0N_1.

Let d_i denote the distance between node $N_i(0 \leq i \leq 6)$ and D_0 and $d_0 \leq d_t$. Then the received power $P_i(0 \leq i \leq 6)$ at node D_0 of the signal from node N_i is equal to

$$P_i = P_0 \left(\frac{d_0}{d_i}\right)^{\gamma} \tag{2}$$

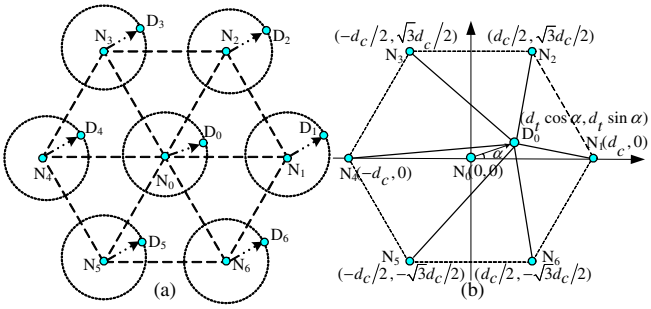

Fig. 1. Interference model

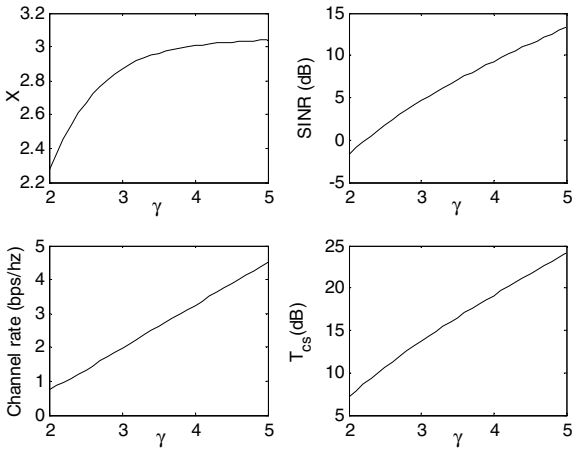

Fig. 2. Carrier sensing threshold with Shanon Capacity

where γ is the path loss exponent and typically $2 \leq \gamma \leq 5$. SINR is equal to

$$SINR = \frac{P_0}{\sum_{i=1}^{6} P_i + P_N} = \frac{1}{\sum_{i=1}^{6} \left(\frac{d_0}{d_i}\right)^{\gamma} + \frac{P_N}{P_0}} \tag{3}$$

where P_N is the noise level and normally it is much less than the power level of the closest interference. It can be shown that when α is in the range $[0, \pi/6]$, SINR is an increasing function of α when $\gamma \geq 2$. Since we consider the worst case, SINR should be calculated at $\alpha = 0$ and $d_0 = d_t$, i.e.,

$$\begin{aligned} \frac{1}{SINR} = & \frac{1}{(X-1)^{\gamma}} + \frac{1}{(X+1)^{\gamma}} + \frac{2}{\left(\left(\frac{X}{2}-1\right)^2 + \left(\frac{\sqrt{3}X}{2}\right)^2\right)^{\frac{\gamma}{2}}} \\ & + \frac{2}{\left(\left(\frac{X}{2}+1\right)^2 + \left(\frac{\sqrt{3}X}{2}\right)^2\right)^{\frac{\gamma}{2}}} + \frac{P_N}{P_0} \end{aligned} \tag{4}$$

Given a requirement of SINR for a coding/modulation scheme and the corresponding achievable channel rate r_c(bps), X is determined. The achievable data rate r_d(bps) equals

$$r_d = \frac{L_{pl}}{T_{preamble} + \frac{L_H + L_{pl}}{r_c}} \tag{5}$$

where $T_{preamble}$ in seconds is a preamble of a packet regardless of the channel rate, such as the physical layer preamble for synchronization purpose at the receiver and the short interframe spacing $SIFS$ at the MAC layer. L_H consists of protocol overheads in bits from different protocol layers, such as MAC and IP layers, and L_{pl} is the size of the payload in bits we wish to transmit.

To calculate the maximum aggregate throughput, we need to know the total number of concurrent transmissions. For a topology with an area of A and with concurrently transmitting pairs as shown in Fig. 1, each transmit-receive pair occupies a nonoverlapping area of $A_0 = \frac{\sqrt{3}}{2} d_c^2$ by ignoring the border effect. For a general topology, A_0 is proportional to d_c^2. Thus the total number of allowed concurrent transmissions is

$$\frac{A}{A_0} \propto \frac{1}{d_c^2} = \frac{1}{d_t^2 X^2} \tag{6}$$

Thus the aggregate throughput S is proportional to

$$S \propto \frac{r_d}{d_t^2 X^2} = \frac{1}{d_t^2 X^2} \frac{L_{pl}}{T_{preamble} + \frac{L_H + L_{pl}}{r_c}} \tag{7}$$

In the following subsections, we will discuss how to select X to maximize the aggregate throughput using Shannon Capacity and the 802.11 data rates, respectively.

Once X is determined, CS_{th} can be set as the power level sensed at distance d_c to guarantee any new concurrent transmission happens at least d_c away. Let T_{cs} denote the ratio of RX_{th} to CS_{th}:

$$T_{cs} = \frac{RX_{th}}{CS_{th}} = X^{\gamma} \tag{8}$$

B. Maximum Throughput and Optimum Carrier Sensing Range under Shannon Capacity

Using Shannon Capacity formula, the achievable channel rate r_c can be obtained given a certain SINR and a bandwidth W(hz):

$$r_c = W \log_2(1 + SINR) \tag{9}$$

$$S \propto \frac{1}{d_t^2 X^2} \frac{L_{pl}}{T_{preamble} + \frac{L_H + L_{pl}}{W \log_2(1+SINR)}} \tag{10}$$

Thus

$$\arg\max_X S = \arg\min_X \left(\frac{T_{preamble} X^2}{L_H + L_{pl}} + \frac{X^2}{W \log_2(1 + SINR)} \right) \tag{11}$$

When X is small, $\log_2(1 + SINR)$ increases along with X and is faster than X^2. When X is large, $\log_2(1 + SINR)$ increases along with X and is slower than X^2. Thus there is an optimum value of X to maximize S. By letting the derivation of Equation (11) with respect to X equal 0, the optimum value of X can be solved given values of $T_{preamble}$, L_H and L_{pl}. The results are shown in Fig. 2 at $T_{preamble} = 0$ and $L_H = 0$.

When $T_{preamble} > 0$ and $L_H > 0$, X and T_{cs} could be smaller. We are not going to further discuss the impact of these protocol overheads on the carrier sensing range under Shannon Capacity. However, as we will discuss below, when the discrete data rates of the standard IEEE 802.11 are considered, the requirement of $SINR$, other than these protocol overheads, plays the major role to determine the optimum carrier sensing range.

TABLE I

SIGNAL-TO-NOISE RATIO AND RECEIVER SENSITIVITY

Rates (Mbps)	SINR (dB)	Receiver sensitivity (dBm)
54	24.56	-65
48	24.05	-66
36	18.80	-70
24	17.04	-74
18	10.79	-77
12	9.03	-79
9	7.78	-81
6	6.02	-82

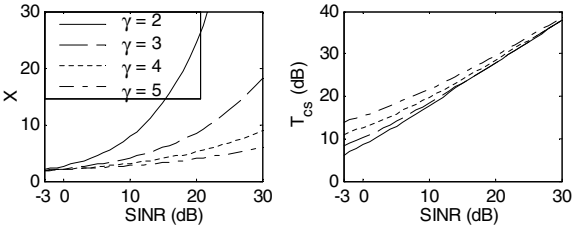

Fig. 3. Carrier sensing threshold with different SINR

C. Maximum Throughput and Optimum Carrier Sensing Range under the Discrete Channel Rates of the IEEE 802.11

For a certain channel rate r_c, there is a requirement of SINR. For example, Table I shows the requirements of SINR of some products for different channel rates [16]. Given the SINR, we can derive the value of X according to Equation (4). Smaller X violates the requirement of SINR and larger X decreases the spatial reuse and the aggregate throughput. Thus, by Equation (7), the protocol overheads $T_{preamble}$ and L_H do not impact the optimum value of X.

The optimum value of X and T_{cs} for different SINR are given in Fig. 3. We also illustrate in Fig. 4 the optimum carrier sensing range for 4 discrete channel rates 6, 18, 36, and 54Mbps with the requirement of SINR in Table I. From the figure, we can observe that the larger the SINR requirement is, the larger X is. X changes in a large range for different values of $SINR$ and so does T_{cs}.

Fortunately, this does not mean that the optimum carrier sensing range changes in a large range because the transmission range and RX_{th} also change in a large range for different channel rates. Table I shows the requirements of receiver sensitivity of the same product for different channel rates. RX_{th} should be larger than or equal to the requirement of receiver sensitivity. This actually represents a common knowledge that higher channel rates sustains in a smaller range for the 802.11 products. The optimum value of carrier sensing threshold CS_{th} can be obtained according to the given RX_{th} and the corresponding optimum value of T_{cs} for a certain channel rate by the following equation,

$$CS_{th} = \frac{RX_{th}}{T_{cs}} \tag{12}$$

Let $i \in \{6, 18, 36, 54\}$ denote the index of $d_c(i)$ and $CS_{th}(i)$ at channel rate 6, 18, 36, and $54Mbps$, respectively.

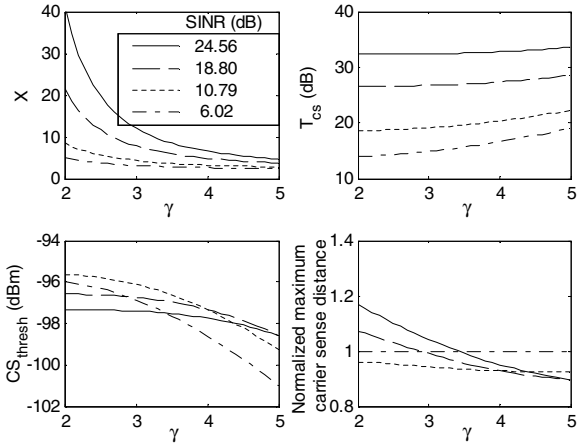

Fig. 4. Carrier sensing threshold with discrete channel rates of 802.11

We define a *normalized maximum carrier sensing distance* as the ratio of $d_c(i)$ to $d_c(6)$, representing the relative size of the optimum carrier sensing range at different channel rates to that at $6Mbps$, and

$$\frac{d_c(i)}{d_c(6)} = \left(\frac{CS_{th}(i)}{CS_{th}(6)}\right)^{\frac{1}{\gamma}} \tag{13}$$

By setting RX_{th} with the value of the receiver sensitivity, we plot CS_{th} and $\frac{d_c(i)}{d_c(6)}$ in Fig. 4. We can observe that although the optimum value of X has a big difference at different channel rates, the carrier sensing threshold and the carrier sensing range does not have much difference for different channel rates and the difference ranges from 0 to 2 dB.

D. Impact of Random Topology

The optimum carrier sensing threshold discussed above only considers a special case, i.e., nodes are always available at the desired location whenever they are needed to make it possible for the scheduled transmissions in Fig. 1. However, the situation rarely happens in practice. First, in a random topology, the possibility that the nodes are located at the desired places is small. Second, even it happens, the chance is still small for all of them successfully contend for the channel for concurrent transmissions. Therefore, considering 6 concurrent interference nodes is too conservative to maximize the spatial reuse in random topology.

Another extreme is to only consider one possibly nearest interference node, like node N_1 to the transmit-receive pair N_0 and D_0 in Fig. 1. The nearest interference distance is $d_c - d_t$, and let X', CS'_{th} and T'_{cs} denote the corresponding X, CS_{th} and T_{cs}, respectively. We have

$$SINR = \left(\frac{d_c - d_t}{d_t}\right)^{\gamma} = (X' - 1)^{\gamma} \tag{14}$$

Given the requirements of $SINR$, we can use the same method as that in Section II-C to derive the carrier sensing threshold CS'_{th} for different channel rates. We have $X' < X$, $CS'_{th} > CS_{th}$ and $T'_{cs} < T_{cs}$. CS'_{th} can be 1 to 6 dB higher than CS_{th}. The corresponding maximum carrier

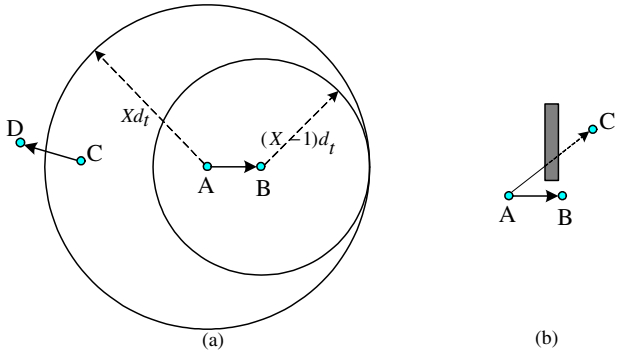

Fig. 5. Tradeoff between exposed terminal problem and hidden terminal problem

sensing distance is 50% to 94%, and the area of carrier sensing range is 25% to 89% of the original values depending on the values of path loss exponent γ and channel rate r_c. Thus a higher carrier sensing threshold CS_{th} may greatly increase the spatial reuse without introducing severe collisions.

E. Tradeoff between Exposed Terminal Problem and the Hidden Terminals Problem

In the analysis of Section II-B and II-C, we have considered all the interference at the worst case to calculate X and CS_{th}. There will be almost no hidden terminal problems, because all interference nodes which may contribute enough interference to corrupt the received packets fall in the carrier sensing range and are required to defer their own transmissions. Notice that the physical carrier sensing does not completely solve the hidden terminal problem. For example in Fig. 5(b), there is an obstruct between node A and C. C may not be able to sense the transmission of A and hence may initiate a new transmission, resulting in a collision at node B.

As we have indicated in the previous subsection that this carrier sensing threshold may be too conservative. Here, we point out another reason that the large carrier sensing range impacts the spatial reuse. As shown in Fig. 5(a), node C's transmission to D will not introduce enough interference to corrupt B's reception. However, node C senses A's transmission and defers its own transmission. This results in poor spatial reuse and is commonly called the exposed terminal problem.

From the point of view of the intended receiver B in Fig. 5(a), we call the range as the *interference range* of B, in which any point has a closer distance to B than $(X-1)d_t$. Any single interference node out of this range may not corrupt B's received packet from A. To measure the impact of the exposed terminal problem, we define an *exposed-area ratio* δ as the ratio of the area of carrier sensing range to that of interference range minus 1 and

$$\delta = \frac{\pi(Xd_t)^2}{\pi((X-1)d_t)^2} - 1 = \left(\frac{X}{X-1}\right)^2 - 1 \qquad (15)$$

It is easy to show that δ decreases from 3 to 0.05 when X increases from 2 to 40. From Fig. 4, we know that a smaller channel rate requires a smaller X and hence a larger exposed-area ratio. And even for the highest channel rate $54Mbps$ allowed in 802.11a/g, the exposed-area ratio cannot be ignored when $\gamma > 3$ because $\delta = 24\%$ and 56% when $X = 10$ and 5, respectively. Let alone that we have not considered a worse case but a common situation in a random topology where the distance between the transmitter and its intended receiver is less than the maximum transmission distance d_t. The interference range should be smaller because the received signal has a greater power. Therefore, the exposed terminal problem cannot be ignored.

Therefore, to alleviate the exposed terminal problem and increase the spatial reuse, it is necessary to decrease the carrier sensing range. However, this may expose a part of the interference range out of the carrier sensing range and results in hidden terminal problem. The smaller the carrier sensing range, the less the exposed terminal problem and the more severe the hidden terminal problem. Apparently, there is a tradeoff between the exposed terminal problem and the hidden terminal problem in order to increase spatial reuse and alleviate the collisions at the same time.

F. Carrier Sensing Range and Strategies for Bidirectional Handshakes

The interference model discussed in Section II focuses on one-way DATA transmissions. However, wireless links are not reliable due to collisions, wireless channel errors and mobility. MAC layer acknowledgements are necessary to check the link reliability and in most cases, link layer retransmissions are more efficient than end-to-end retransmissions for such unreliable links. Besides, the bidirectional handshake has already been adopted by the IEEE 802.11 MAC protocols which define a two-way DATA/ACK handshake and a four-way RTS/CTS/DATA/ACK handshake for each data packet transmission. Therefore, the receivers may also transmit CTS/ACK and the interference at node D_0 in Fig. 1 becomes worse, hence the original interference model in Equation (3) is not always effective to avoid the collisions.

When bidirectional handshakes are considered, the following three problems have not been well addressed in that interference model. The first problem is the packet collision. The second one is the receiver blocking problem [17], [18]. This problem describes the situation that the transmitter keeps (re)transmitting RTS or DATA frames when the intended receiver senses a busy channel due to other ongoing transmissions and does not or cannot respond with CTS or ACK frames. After the retransmission times exceeds a certain threshold [1], the transmitter will drop the data packet, declare the link failure and hence route repair will be executed. We call this receiver as a blocked receiver. The third one is unfairness resulting from the previous two problems.

These problems are related with the carrier sensing strategies. There are largely two carrier sensing strategies in the IEEE 802.11. The *strategy I* is to forbid a node from transmitting if it senses a busy channel. The *strategy II* is to allow a node to transmit at any situations even if it senses

a busy channel. In the 802.11, the first strategy is adopted for transmissions of RTS, DATA and CTS frames. The second one is adopted for transmissions of ACK frames to acknowledge the successfully transmitted DATA frames.

We use a simple topology to illustrate these problems, i.e., the linear topology A—— B $\cdots\cdots$ C —— D. We first discuss the packet collision problem. Suppose D cannot sense A's transmission and is out of B's interference range. However, C is close enough to B so that C(or B)'s transmission will corrupt B(or C)'s reception. When A is transmitting to B, D may initiate a transmission to C. And it is the same for A when D is transmitting to C. If one or both of A and D are transmitting DATA frames, B or C, which first finishes the reception of the DATA frame, will return an ACK frame which does not require carrier sensing beforehand and will corrupt the reception at the other. To alleviate this problem, we may propose to use the short frames RTS/CTS before DATA/ACK since CTS requires carrier sensing beforehand. However, the carrier sensing strategy of CTS frames makes the receiver blocking problem worse.

The receiver blocking problem exists when the intended receiver does not return an ACK frame due to a collision. It also exists for the carrier sensing strategy I even when the intended receiver can correctly decode the received packet but could not respond due to the carrier sense rule. For example in the previous topology, suppose that A and C are out of each other's sensing range, and B and C are out of each other's interference range and cannot corrupt each other's received packets. However, B and C can sense each other's transmission. When C is transmitting a long DATA frame to D, A may initiate a transmission to B by a RTS frame. Since B senses a busy channel, it does not return a CTS frame so that A keeps retransmitting the RTS frame. A also doubles its contention window size for each failure of RTS transmission and has lower channel access probability. If C has a lot of data packets destined to D and occupies the channel for a long time, A will be starved. Apparently this is unfair to A due to the MAC contention.

To alleviate these problems as much as possible for the bidirectional handshakes, it is necessary to be more conservative to set the carrier sensing range than the interference model in Fig. 1 especially for the interference model at the worst case. First, to address the packet collision problem, we need to consider the interferences from node D_i $(1 \le i \le 6)$ which can be at most d_t closer to D_0 than N_i. Denote the new value of X as $\widehat{X}$. Following the similar procedures in Section II-A, the SINR at the worst case satisfies

$$\frac{1}{SINR} = \frac{1}{(\widehat{X}-2)^{\gamma}} + \frac{1}{\widehat{X}^{\gamma}} + \frac{2}{\left(\sqrt{\left(\frac{\widehat{X}}{2}-1\right)^2+\left(\frac{\sqrt{3}\widehat{X}}{2}\right)^2}-1\right)^{\gamma}} + \frac{2}{\left(\sqrt{\left(\frac{\widehat{X}}{2}+1\right)^2+\left(\frac{\sqrt{3}\widehat{X}}{2}\right)^2}-1\right)^{\gamma}} + \frac{P_N}{P_0} \tag{16}$$

The numerical results show that $\widehat{X}$ can be well approximated by $X+1$ with less than 1% error when SINR is larger than -3dB:

$$\widehat{X} \cong X+1 \tag{17}$$

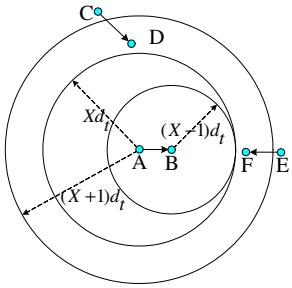

Fig. 6. Large carrier sensing range with carrier sensing strategy II for CTS/ACK

For example in the previous four-node topology, the two receivers B and C are thus far enough from each other and the ACK frames cannot corrupt each other's reception. Second, when RTS/CTS are used, using the carrier sensing strategy II for CTS/DATA/ACK frames to address the receiver blocking problem and RTS still adopts the carrier sensing strategy I. For example in the same topology as before, B is far enough from the transmitting node C and can correctly decode a RTS or DATA frame from A. Moreover, it does not prevent from returning a CTS or ACK frame. The new carrier sensing range is shown in Fig. 6.

Apparently, the cost is to aggravate the exposed terminal problem and sacrifice the spatial reuse in a more general topology. However, the packet collision and dropping due to hidden terminals and blocked receivers have been significantly improved. Moreover we expect a more stable performance for higher layer protocols, such as much less retransmission and timeouts for TCP traffic, and much less false link failures and unnecessary rerouting activities, and the unfairness due to these two problems can also be greatly alleviated.

Other problems for the large carrier sensing range are as follows. First, it requires a small sensing threshold. We do not know the achievable carrier sensing sensitivity of the current products. In the following studies, we assume that the current products or future technologies could support the small carrier sensing threshold, i.e., T_{lcs} times more sensitive than the original value. The new value of T_{cs} is $\widehat{T_{cs}}$ and equals

$$\widehat{T_{cs}} = T_{cs}/T_{lcs}, \qquad T_{lcs} = (\frac{\widehat{X}}{X})^{\gamma} \tag{18}$$

When $\gamma = 3$, $T_{lcs} = 5.28, 3.75$ and $2.91dB$ for $X = 2, 3$ and 4, respectively. Second, the larger carrier sensing range means that there may exist more nodes contending for the shared channel. The collision probability like that in wireless LANs increases with the number of active nodes [19], [20].

To address the collision problem in one carrier sensing range, there are already several methods. First, four-way handshake instead of two-way handshake could be used to reduce the long collision periods of DATA frame transmissions if the collision probability is high and the DATA frame is

long. Second, some schemes [21]–[26] controlling the traffic delivered to the MAC layer according to the channel status can be used to efficiently reduce the collision probability. Third, we can maintain the value of X but reduce both the carrier sensing range and transmission range in order to reduce the node density in each carrier sensing range.

G. Optimum Carrier Sensing Range

In short, large carrier sensing range with appropriate sensing strategies for different MAC frames can efficiently address the hidden terminal problem and receiver blocking problem but aggravate the exposed terminal problem and decrease the spatial reuse. The optimum carrier sensing range with a radius $d_c^* = X^* d_t$ must balance the impact of both collisions and spatial reuse, where

$$X^* = \mu\widehat{X} = \mu(X+1)(0 < \mu \leq 1) \tag{19}$$

Simulation studies with considerations of all previously aforementioned factors will be conducted in Section IV to identify the optimum value of carrier sensing threshold.

III. Utilize Multirate Capability of 802.11 in Wireless Multihop Ad Hoc Networks

In this section, we study the impact of multihop forwarding on the optimum carrier sensing threshold as well as how to maximize the spatial reuse ratio for multihop flows when multiple rates coexist in wireless multihop ad hoc networks. Different from the previous section where the objective is to maximize the aggregate one-hop throughput, the end-to-end performance in terms of delay, throughput and energy consumption of multihop flows deserves more attention. We first discuss how to set the carrier sensing threshold for a multirate wireless ad hoc networks. Then we study the impact of different channel rates on the end-to-end performance. According to the analysis and the carrier sensing model in the previous section, the optimum end-to-end throughput and the corresponding carrier sensing threshold are derived for a multihop flow. Finally we propose to utilize the bandwidth distance product as a metric to determine the forwarding nodes of multihop flows to maximize the spatial reuse ratio when multiple rates coexist.

A. How to Set the Carrier Sensing Threshold for Multirate 802.11 MAC protocol

In this paper, we argue that the multirate 802.11 MAC protocol should adopt a single carrier sensing threshold for all channel rates for three reasons. First, a single carrier sensing threshold keeps the Physical/MAC protocols simple. The achievable channel rate is subject to distance, mobility and channel fading and is time variable. Hence multiple carrier sensing thresholds for different channel rates may greatly increase the complexity of the protocols. Second, as discussed above, the optimum carrier sensing thresholds do not change much for different channel rates. A single threshold will not sacrifice the performance much. Third, multiple carrier sensing thresholds may introduce additional collisions. For example in Fig. 7, a transmit-receive pair A and B, which have a large carrier sensing range corresponding to a certain channel rate, senses an idle channel and then A transmits the DATA frames. During the transmission period, another transmitter C in the previous transmitter's sensing range also senses an idle channel due to a smaller carrier sensing range. The new transmission from C may introduce a collision at the previous intended receiver B.

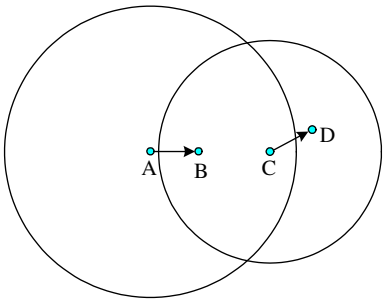

Fig. 7. Multiple carrier sensing thresholds may result in collisions

With a common carrier sensing threshold, the receive threshold RX_{th} must be set appropriately. First, RX_{th} must be larger than or equal to the receiver sensitivity RX_{se} required by the adopted channel rate. Second, to alleviate collisions as much as possible, one more requirement may be enforced, i.e., the power level of the received signal must be larger than or equal to $CS_{th}T_{cs}$. According to these two requirements, we can set the common carrier sensing threshold CS_{th}^* as

$$\begin{aligned} CS_{th}^* &= \max\left(\tfrac{RX_{se}(i)}{T_{cs}(i)}\right) \\ RX_{th}(i) &= CS_{th}^* T_{cs}(i) \geq RX_{se}(i) \end{aligned} \tag{20}$$

where i is the index of different channel rates.

B. How to Choose Next hops, Channel Rates and Set the Carrier Sensing Threshold for Multihop Flows

For a single hop network like a wireless LAN, it seems simple to maximize the end-to-end throughput and minimize the end-to-end delay for a flow. The solution is just to use the highest achievable channel rate between the source and the destination. However, if there exist some users far away from the access point or their intended receivers, only very low channel rates are available. Deploying a relay access point at an appropriate place or utilizing another user as a forwarding node can utilize higher channel rates over multiple hops instead of a low channel rate over one single hop and hence may achieve much better performance.

In wireless multihop ad hoc networks, destinations are often out of the sources' transmission range and packets need to be forwarded through multiple hops before reaching the destinations. Selecting the next hop with the highest channel rate can increase the throughput at each hop. However, packets must travel through more hops due to the short transmission range of high channel rates and hence the end-to-end delay and throughput are not necessarily improved. To determine the best candidate of the next hop, it is necessary to introduce

a metric consisting of information of both channel rates and hop distances.

1) End-to-end transmission delay and energy efficiency

Suppose there is a perfect packet scheduling algorithm. Queueing delay is equal to zero and the MAC layer backoff period is also decreased to a minimum value and can be ignored. Thus the end-to-end delay t_{e2e} is equal to the summation of transmission delay t_h at all hops.

$$t_{e2e} = \sum_{\text{i} \in \{\text{all hops}\}} t_h(i) \tag{21}$$

where i is the index of hops along the path. And the hop transmission delay t_h is

$$t_h = T_{preamble} + \frac{L_H + L_{pl}}{r_c} \tag{22}$$

Suppose RTS/CTS/ACK are transmitted with the basic rate and DATA is transmitted with the selected channel rate r_c, then

$$\begin{aligned} T_{preamble} &= (T_{RTS} + T_{CTS} + 2T_{SIFS})\varphi + \\ &\quad SIFS + DIFS + 2T_{phy} + T_{ACK} \\ \varphi &= \begin{cases} 1, \text{(if RTS/CTS are used)} \\ 0, \text{(if RTS/CTS are not used)} \end{cases} \end{aligned} \tag{23}$$

To determine the efficiency of each hop (or that of the candidates at each hop), we define a *bandwidth distance product* BDiP for each hop as the achievable data rate r_d times the hop distance d_h at that hop, then

$$BDiP = r_d \times d_h = \frac{L_{pl}}{T_{preamble} + \frac{L_H + L_{pl}}{r_c}} d_h \tag{24}$$

The *per meter transmission delay* t_m for the hop is equal to

$$t_m = \frac{t_h}{d_h} = \frac{L_{pl}}{BDiP} \tag{25}$$

End-to-end delay is the summation of transmission delay at all forwarding nodes. If the path is a regular chain where each hop has the same distance and the total path length is d_p, then the end-to-end transmission delay t_{e2e} is equal to

$$t_{e2e} = t_m d_p = \frac{L_{pl} d_p}{BDiP} \tag{26}$$

Normally, d_p is proportional to the distance d_{sd} between the source and the destination. Suppose it has a relatively fixed value, then the end-to-end delay is inversely proportional to the bandwidth distance product BDiP.

In this paper, we assume a common transmission power P_t for all channel rates. Thus the aggregate transmission power consumption E for each packet is

$$E = P_t \times \sum_{\text{i} \in \{\text{all hops}\}} (t_h(i) - T_{SIFS} - T_{DIFS} - 2\varphi T_{SIFS}) \tag{27}$$

Since T_{SIFS} and T_{DIFS} are much smaller than T_{DATA}, minimizing the end-to-end delay is almost equivalent to minimizing the end-to-end energy consumption E.

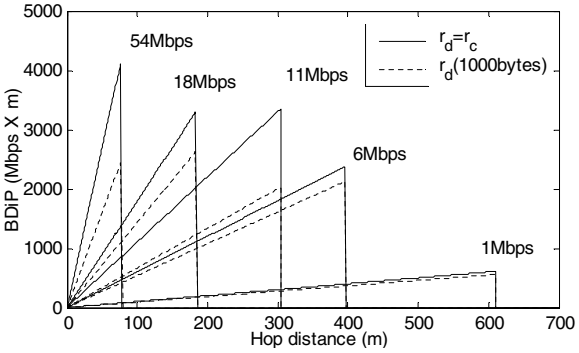

Fig. 8. Bandwidth distance product

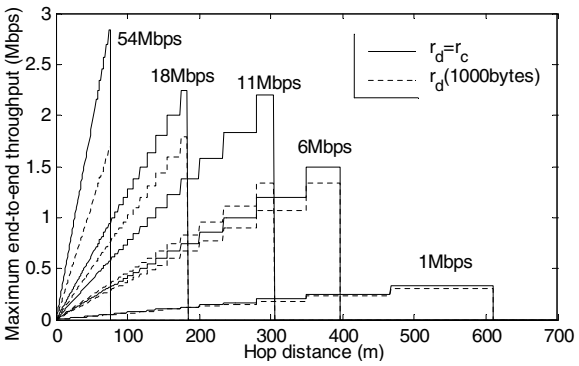

Fig. 9. Maximum end-to-end throughput for different hop distance

Therefore, to minimize the end-to-end delay and energy consumption, we should select the candidate with the highest value of BDiP as the next hop if other conditions are the same. Fig. 8 shows the bandwidth distance product for several channel rates. To plot the figure, the advertised transmission ranges for outdoor environments of one Cisco product [27] are used. They are 76, 183, 304, 396, and 610m for 54, 18, 11, 6, and 1Mbps respectively. Notice that 1 and 11Mbps are the 802.11b rates and 6, 18 and 54Mbps are the 802.11g rates. We use the default parameters defined for the 802.11b/g rates according to the corresponding standards [28] and [29], respectively (802.11g rates have shorter preambles). Two cases are considered with and without protocol overheads. For the case without protocol overheads, $r_d = r_c$. For the case with protocol overheads, two-way handshake DATA/ACK and 1000 bytes payload size are used.

Two important observations can be found from Fig. 8. First, larger protocol overheads result in smaller BDiP. Second, higher channel rates do not necessarily generate larger BDiP. The maximum value of BDiP is closely related to both hop distance and protocol overheads in addition to the achievable channel rate.

2) End-to-end throughput and spatial reuse

In wired networks, the maximum end-to-end throughput of one multihop flow can be determined by the bottleneck link with the smallest available bandwidth for the flow. However, the issue becomes much more complex due to the shared

channel in wireless networks. We must consider channel rate, transmission distance at each hop as well as the carrier sensing range and spatial reuse.

To maximize the end-to-end throughput of a multihop flow, it is necessary to maximize the spatial reuse along the path, i.e., to schedule as many concurrent transmissions at different hops as possible. There are two requirements to schedule successful concurrent transmissions. First, two neighboring transmitters along the path must be at least d_c away from each other so that there is only one transmitter in each carrier sensing range to satisfy the carrier sensing requirement. Second, the concurrent transmissions at upstream and downstream nodes cannot introduce enough interference to corrupt the reception at the considered transmit-receive pair.

Let $\frac{1}{N}$ denote the *spatial reuse ratio of a multihop flow* where N is the hop distance between two nearest concurrent and successful transmissions along the path, and

$$N \geq \lceil \frac{d_c}{d_h} \rceil \tag{28}$$

where $\lceil x \rceil$ is the ceiling function of x and is equal to the nearest integer greater than or equal to x. Thus, for a chain topology with a common distance d_h at each hop, the maximum end-to-end throughput for a multihop flow with at least N hops is

$$S_{max} = \frac{r_d}{N} \leq \frac{r_d}{\lceil \frac{d_c}{d_h} \rceil} \tag{29}$$

because there can be only one successful transmission in each N hops and hence the spatial reuse ratio for the chain topology is $\frac{1}{N}$.

The equality in the above two inequalities holds only when the carrier sensing range is set to satisfy the second requirement discussed above. That is to say, there should be no hidden terminal problem or receiver blocking problem as discussed in Section II-F due to the transmission at N hops away along the path. This maximum end-to-end throughput is shown in Fig. 9, where we suppose $d_c = 1400m$ is the minimum value to satisfy the above requirements. When protocol overheads are considered and 1000bytes payload is used, S_{max} equals to 1.68, 1.79, 1.33, 1.34, 0.30Mbps for 54, 18, 11, 6, 1Mbps at their corresponding maximum hop distance, respectively. It verifies that higher channel rates do not necessarily generate higher end-to-end throughput. It is closely related to the achievable channel rate, hop distance, carrier sensing range and protocol overheads.

As discussed in Section II, the optimum carrier sensing range may allow a certain level of hidden terminal problem to balance the impact of exposed terminal problem. In this case, Equations (28) and (29) only provide a lower bound for N and an upper bound for the maximum end-to-end throughput. To accurately calculate the maximum end-to-end throughput, N should be recalculated with the requirement that the concurrent scheduled transmissions should not introduce enough interference to each other to corrupt the receptions. Thus, N is determined by the requirement of SINR and the locations of the sources and forwarding nodes. Here we use

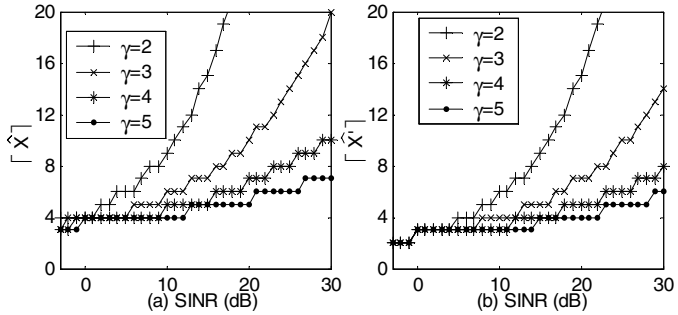

Fig. 10. Spatial reuse ratio for multihop flows (a) at worst case, (b) in a single chain topology with one way traffic

the interference model used in Equation (16) for the worst case with bidirectional handshakes, and

$$N \leq \lceil \widehat{X} \frac{d_t}{d_h} \rceil, (d_h \leq d_t) \tag{30}$$

$$S_{max} \geq \frac{r_d}{\lceil \widehat{X} \frac{d_t}{d_h} \rceil}, (d_h \leq d_t) \tag{31}$$

If all hop distances equal the same value or the hop distances are set as d_h, these two equations can be simplified as $N \leq \lceil \widehat{X} \rceil$ and $S_{max} \geq \frac{r_d}{\lceil \widehat{X} \rceil}$, and $\frac{r_d}{\lceil \widehat{X} \rceil}$ is the maximum achievable end-to-end throughput for a multihop flow with at least $\lceil \widehat{X} \rceil$ hops under the used interference model. Thus, $\lceil \widehat{X} \rceil$ can represent the spatial reuse ratio for multihop flows.

Generally, there are less interferences than the worst case. For a regular chain topology with a common hop distance, if we only consider the interference from one nearest upstream transmission and one nearest downstream transmission, and let $\widehat{X'}$ denote the value of $\widehat{X}$, Equation (16) becomes

$$\frac{1}{SINR} = \begin{cases} \frac{1}{(\widehat{X'}-1)^\gamma} + \frac{1}{\widehat{X'}^\gamma} + \frac{P_N}{P_0} \text{(one way traffic)} \\ \frac{1}{(\widehat{X'}-2)^\gamma} + \frac{1}{\widehat{X'}^\gamma} + \frac{P_N}{P_0} \text{(two way traffic)} \end{cases} \tag{32}$$

where SINR is worse for the case of two-way traffic because the receiver of the concurrent downstream transmission can be closer than its intended transmitter to the considered receiver. Thus the aggregate end-to-end throughput for two way traffic can be lower than one-way traffic. However, if an optimum packet scheduler is possible to schedule forwarding traffic at one time and reverse traffic at another time, the aggregate end-to-end throughput of two way traffic can be as high as that of one way traffic. Thus only the case of one-way traffic is discussed thereafter.

Since a smaller value of X than $\widehat{X'}$ dose not help increase the throughput due to the requirement of SINR and only results in collisions due to the hidden terminal problem. Therefore, $\widehat{X'}$ is the optimum value of X for a multihop flow in a regular chain topology and

$$\begin{aligned} N &= \lceil \widehat{X'} \frac{d_t}{d_h} \rceil \geq \lceil \widehat{X'} \rceil, (d_h \leq d_t) \\ S_{max} &= \frac{r_d}{\lceil \widehat{X'} \frac{d_t}{d_h} \rceil} \leq \frac{r_d}{\lceil \widehat{X'} \rceil}, (d_h \leq d_t) \end{aligned} \tag{33}$$

Therefore the achievable maximum end-to-end throughput of a multihop flow is $\frac{r_d}{\lceil \widehat{X'} \rceil}$ when $d_h = d_t$. Notice that $\widehat{X'}$ may not be the optimum value of X that should satisfy $X \leq \widehat{X}$ in a general topology, and depends on many factors as we have discussed in Section II.

Fig. 10 shows both $\widehat{X}$ and $\widehat{X'}$ along with different requirement of SINR. When SINR = 10dB and $\gamma = 4$(for distant field) which are the default settings in ns2, the spatial reuse ratio is $\frac{1}{3}$ and hence the maximum end-to-end throughput is $\frac{1}{3}$ of the bandwidth for a chain topology with at least 3 hops. This is larger than the findings in [2] and [5] which shows the spatial reuse ratio is $\frac{1}{4}$. There are two reasons for the throughput loss. First, these papers study the four-way handshake RTS/CTS/DATA/ACK and the throughput suffers from the receiver blocking problem as we discussed in Section II-F. Second, these papers use ns2 for simulation studies and a MAC frame is discarded if there is already an interference when receiving the first bit of the frame even when SINR is high enough in the current version of ns2. Fig. 10 also shows that larger γ can achieve better spatial reuse ratio and hence higher end-to-end throughput because the interference vanishes more quickly along with the distance. However, larger γ results in shorter transmission distance, and hence requires more forwardings and consumes more energy for each packet to reach the destination.

Furthermore, S_{max} in the above equations only consider multihop flows with at least N hops. For a multihop flow with fewer hops, we have

$$S_{max} = \frac{r_d}{n_h} (n_h \leq N) \tag{34}$$

where n_h is the number of hops of the multihop flow.

In short, to maximize the end-to-end throughput of a multihop flow, it is necessary to select a node with the highest value of $\frac{r_d}{N}$ as the downstream forwarding node if other conditions are the same. The optimum value of N depends on the locations of interfering transmitters and hence is not easy to calculate for an irregular topology. However, we know that the optimum value of carrier sensing distance $d_c = X d_t$ for different channel rates does not have much difference. From Equation (33), we can see that S_{max} is approximately proportionally to the bandwidth distance product $BDiP = r_d d_h$. Thus $BDiP$ can be utilized to approximately represent the efficiency of throughput, delay and energy consumption at each hop. We will evaluate the efficiency of this metric to maximize the end-to-end throughput and compare it with the shortest hop algorithm for a multirate network through simulations in next section.

IV. Simulation Studies

In this section, we conduct ns2 simulations to study the impact of carrier sensing range on the system performance and to identify the optimum carrier sensing range. We also illustrate that how the carrier sensing range and spatial reuse impact the maximum throughput of multihop flows and how the bandwidth distance product is used as a metric to select the forwarding nodes to optimize the performance in a multirate network.

A. ns2 extensions and simulation setup

We have developed several important extensions to ns2 to obtain more accurate results. First, the interferences are added up instead of checking them one by one when determining the SINR. Second, the incoming signal is regarded decodable even when the node senses a busy channel at time instant of the first bit of the incoming frame if the SINR is high enough. Originally, ns2 only considers the capture effect when the interference comes after the intended signal. Third, ns2 is extended to support multiple channel rates, i.e., the MAC layer has the appropriate settings of a SINR requirement, a receiver threshold and a transmission range for each channel rate. Fourth, the extensions provide an option not to sense the channel before sending a CTS or a DATA frame to a correctly received RTS or CTS frame when RTS/CTS are used. Originally, ns2 discards a successfully received RTS frame if the channel is sensed busy. We denote this option as *CSSII* (carrier sensing strategy II as discussed in Section II-F) in the following subsections.

We adopt the requirements of SINR and receiver sensitivities in Table I unless otherwise indicated, and the receiver threshold is set as the value of the corresponding receiver sensitivity for each channel rate. The default two ray ground propagation model in ns2 is used, i.e., the path loss exponent $\gamma = 2$ when the distance is less than 86m and $\gamma = 4$ otherwise, and the transmit power is set as 6dBm. The transmission ranges are hence determined. In the simulations, the channel rates 54, 36, 18, and 6Mbps are studied, and their transmission radii are 89, 119, 178, and 238m, respectively. The IEEE 802.11a [30] protocol parameters are adopted in the simulations.

B. Optimum carrier sensing range

In this subsection, we try to identify the optimum carrier sensing range. In the simulations, there are total 150 nodes randomly distributed in a 1000m $\times$ 1000m topology.

First we identify the optimum carrier sensing threshold CS_{th} for one-hop flows. In the simulation, each node randomly selects one neighbor as the destination of one TCP connection. Notice that the neighborhood is smaller for a higher channel rate due to its smaller transmission range. Fig. 11 shows that the aggregate throughput achieves the maximum value when CS_{th} is in the range of $[61, 76]$dBm for all channel rates. However, such CS_{th} is even less than RX_{th} for several channel rates. Apparently, it starves the flows whose source destination distance is close to the transmission radius as found from the more detailed simulation results.

We also identify the optimum carrier sensing threshold CS_{th} if multihop flows exist. In the simulation, there are total 20 TCP connections. The sources and the destinations are randomly selected under the condition that the distance between the source and the destination ranges from 500 to 600m. The distance condition is used instead of the hop

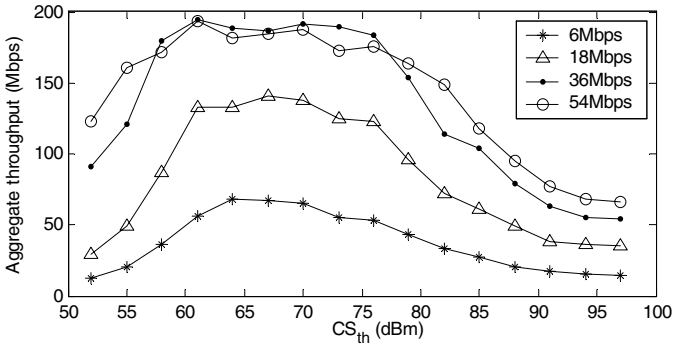

Fig. 11. Optimum carrier sensing threshold for one-hop flows

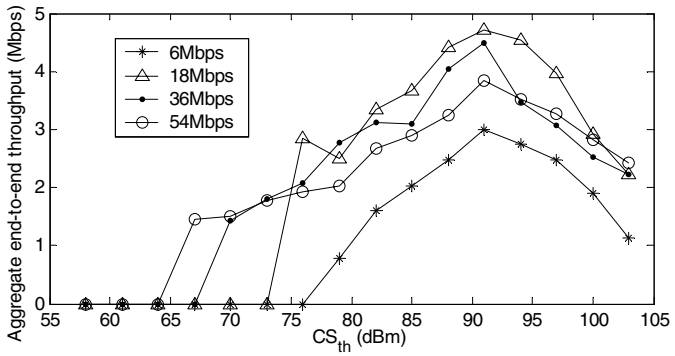

Fig. 12. Optimum carrier sensing threshold for multi-hop flows

number because we also want to check the efficiency of different channel rates to deliver traffic over the same distance and higher channel rates often travel more hops to reach the same destination. Fig. 12 shows that the aggregate end-to-end throughput achieves the maximum value when CS_{th} is around 91dBm for all channel rates. When the CS_{th} is less than the receiver threshold RX_{th}, the end-to-end throughput is almost zero. This is because that some hop distances approach the maximum transmission distance, which leads to disconnections of these hops.

There are several important observations from these results. First, to determine the optimum carrier sensing range in the multihop ad hoc networks, it is not enough to examine the performance of one-hop flows and the impact of multihop forwarding must be carefully studied. Second, a single carrier sensing threshold could be optimum for all channel rates. Third, a higher channel rate does not necessarily generate a higher throughput. We must be careful to utilize the multirate capability in the multihop environment which will be further studied in next subsection. These observations verify our earlier analytical results in this paper.

C. Spatial reuse and end-to-end performance of multihop flows

In this subsection, we first verify that the maximum spatial reuse ratio of a regular chain topology is $\frac{1}{3}$ instead of $\frac{1}{4}$ using the default parameters of ns2 where the SINR requirement is 10dB. The hop distance is set as the maximum transmission distance and the channel data rate is 6Mbps. The maximum throughput is found by gradually increasing the carrier sensing threshold and the rate of CBR traffic from the source. As long as $12dB < \frac{RX_{th}}{CS_{th}} < 19dB$, i.e., $2 < X < 3$, the maximum throughput can be achieved. Larger CS_{th} results in more collisions due to the hidden terminal problem and hence lower throughput. Smaller CS_{th} results in lower spatial reuse ratio, hence lower throughput. When two-way handshake DATA/ACK is used, the maximum end-to-end throughputs are 5.17, 2.52, 1.71, 1.68, 1.68, 1.68, 1.67, 1.67Mbps for 1 to 8 hops regular chain topologies, respectively. When four-way handshake RTS/CTS/DATA/ACK and CSSII are used, they are 4.95, 2.41, 1.63, 1.61, 1.61, 1.61, 1.60, 1.59Mbps respectively. It verifies that the maximum end-to-end throughput of a multihop flow with at least 3 hops is $\frac{1}{3}$ of the one-hop flow's throughput with the 10dB SINR requirement. The slightly decreasing throughputs are due to the increasing impact of randomness of the backoff periods on the packet scheduling at the MAC layer along with the chain length. Thus, the results verify that $\frac{1}{3}$ instead of $\frac{1}{4}$ is the optimum spatial reuse ratio for the simulated settings. $\frac{1}{4}$ obtained in other papers is due to the receiver blocking problem, ns2 implementation and carrier sensing strategy used by the IEEE 802.11 protocols as discussed in Section III.

To check the efficiency of bandwidth distance product BDiP on maximizing the spatial reuse ratio and hence optimizing the end-to-end performance of multihop flows, we also simulate a random chain topology. In the topology, there are total 30 nodes. The distance between the source and the distance is 2000 meters. Other 28 nodes are randomly distributed between the source and the destination. Three algorithms in determining forwarding nodes and the channel rates are compared with each other. The first one is similar to the shortest hop algorithm, i.e., selecting the farthest reachable node and using the highest achievable rate between this node and the transmitter. The second one selects the farthest node among those with a same highest channel rate as the forwarding node. The third one selects the node with the highest value of BDiP as the downstream forwarding node at each hop. They are referred as $\mathbf{A_{dr}}$ (first consider the distance, then the rate), $\mathbf{A_{rd}}$ (first consider the rate, then the distance) and $\mathbf{A_{BDiP}}$ (maximize the bandwidth distance product), respectively, in the following discussions.

The maximum end-to-end throughputs are achieved when $\frac{P_t}{CS_{th}}$ is around 97$\sim$101dB ($CS_{th} = 91 \sim 95dBm$) for all three algorithms, and they are 1.64, 1.87 and 2.08Mbps for $\mathbf{A_{dr}}$, $\mathbf{A_{rd}}$ and $\mathbf{A_{BDiP}}$, respectively. The improvement of $\mathbf{A_{rd}}$ and $\mathbf{A_{BDiP}}$ over $\mathbf{A_{dr}}$ are 14% and 27%, respectively. Notice that these simple algorithms are only used to show the advantages of bandwidth distance product as a routing metric. Similar to bandwidth, bandwidth distance product is a link-based metric. Therefore, some more sophisticate routing algorithms, such as the widest path routing algorithm, can be adopted to use it as a routing metric to route around obstacles and to compute a loop-free path in a more general topology.

V. Conclusions

In this paper, we analyze the impact of several important factors on the optimum carrier sensing threshold in the multirate and multihop wireless ad hoc networks. Several key observations are listed as follows:

- Multihop property must be considered to decide the optimum carrier sensing threshold. The optimum carrier sensing threshold for one-hop flows does not work for multihop flows.
- Different channel rates have similar optimal carrier sensing thresholds. Therefore, a single carrier sensing threshold for different rates could be efficient as well as simple.
- Higher channel data rate does not necessarily generate higher throughput. We need to be careful to utilize the multirate capability.
- Shortest hop routing algorithm is not appropriate for multirate and multihop wireless ad hoc networks. Simulation results show that the algorithms $\mathbf{A_{rd}}$ (first consider the rate, then the distance) and $\mathbf{A_{BDiP}}$ (maximize the bandwidth distance product) can improve the throughput by 14% and 27%, respectively. Hence, the results demonstrate that bandwidth distance product could be a good routing metric in multirate ad hoc networks.
- Maximum end-to-end throughput is derived for a multihop flow under a certain requirement of SINR. The maximum throughput can be achieved only when the carrier sensing threshold is appropriately set. Current ns2 version fails to do so. Several ns2 extensions have been developed to achieve the maximum throughput. For example, the maximum spatial reuse ratio of a multihop flow is $\frac{1}{3}$ instead of $\frac{1}{4}$ for the 10dB SINR requirement.

References

[1] *IEEE standard for wireless LAN medium access control (MAC) and physical layer (PHY) specifications, ISO/IEC 802-11: 1999(E)*, Aug. 1999.

[2] J. Li, C. Blake, D. S. J. De Couto, H. I. Lee, and R. Morris, "Capacity of ad hoc wireless networks," in *Proc. ACM MobiCom*, July 2001.

[3] X. Chen, H. Zhai, J. Wang, and Y. Fang, "TCP performance over mobile ad hoc networks," *Canadian Journal of Electrical and Computer Engineering (CJECE) (Special Issue on Advances in Wireless Communications and Networking)*, vol. 29, pp. 129–134, 2004.

[4] H. Zhai, X. Chen, and Y. Fang, "Rate-based transport control for mobile ad hoc networks," in *Proc. of IEEE Wireless Communications and Networking Conference (WCNC'05)*, March 2005.

[5] H. Zhai, J. Wang, and Y. Fang, "Distributed packet scheduling for multihop flows in ad hoc networks," in *Proc. IEEE WCNC*, March 2004.

[6] H. Zhai, X. Chen, and Y. Fang, "Alleviating intra-flow and inter-flow contentions for reliable service in mobile ad hoc networks," in *Proc. of IEEE Military Communications Conference (Milcom'04)*, Nov. 2004.

[7] K. Xu, M. Gerla, and S. Bae, "How effective is the IEEE 802.11 RTS/CTS handshake in ad hoc networks?" in *Proc. IEEE GlobeCom*, 2002.

[8] P. Gupta and P. R. Kumar, "The capacity of wireless networks," *IEEE Transactions on Information Theory*, vol. 46, pp. 388–404, 2000.

[9] R. Hekmat and P. V. Mieghem, "Interference in wireless multi-hop ad-hoc networks and its effect on network capacity," in *Med-hoc-Net*, September 2002.

[10] X. Guo, S. Roy, and W. S. Conner, "Spatial reuse in wireless ad-hoc networks," in *Proc. VTC*, 2003.

[11] S. Gobriel, R. Melhem, and D. Mosse, "A unified interference/collision analysis for power-aware adhoc networks,?" in *Proc. Infocom*, March 2004.

[12] Z. Li, S. Nandi, and A. K. Gupta, "Improving MAC performance in wireless ad hoc networks using enhanced carrier sensing (ECS)," in *Third IFIP Networking*, 2004.

[13] J. Deng, B. Liang, and P. K. Varshney, "Tuning the carrier sensing range of IEEE 802.11 MAC," in *Proc. IEEE GLOBECOM*, Dec. 2004.

[14] J. Zhu, X. Guo, L. L. Yang, and W. S. Conner, "Leveraging spatial reuse in 802.11 mesh networks with enhanced physical carrier sensing," in *Proc. IEEE ICC*, June 2004.

[15] X. Yang and N. H. Vaidya, "On the physical carrier sense in wireless ad hoc networks," in *Proc. IEEE Infocom*, March 2005.

[16] J. Yee and H. Pezeshki-Esfahani, "Understanding wireless LAN performance trade-offs." CommsDesign.com, Nov. 2002.

[17] H. Zhai, J. Wang, Y. Fang, and D. Wu, "A dual-channel MAC protocol for mobile ad hoc networks," in *IEEE Workshop on Wireless Ad Hoc and Sensor Networks, in conjuction with IEEE Globecom 2004*, Nov. 2004.

[18] H. Zhai, J. Wang, and Y. Fang, "Ducha: A dual-channel MAC protocol for mobile ad hoc networks," *to appear in IEEE Transactions on Wireless Communications*, 2005.

[19] H. Zhai, Y. Kwon, and Y. Fang, "Performance analysis of IEEE 802.11 MAC protocols in wireless LANs," *Wireless Communications and Mobile Computing,*, vol. 4, pp. 917–931, 2004.

[20] H. Zhai and Y. Fang, "Performance of wireless LANs based on IEEE 802.11 MAC protocols," in *Proc. of IEEE International Symposium on Personal, Indoor and Mobile Radio Communications (PIMRC'03)*, September 2003.

[21] H. Zhai, X. Chen, and Y. Fang, "A call admission and rate control scheme for multimedia support over IEEE 802.11 wireless LANs," *to appear in ACM Wireless Networks*, 2005.

[22] ——, "A call admission and rate control scheme for multimedia support over IEEE 802.11 wireless LANs," in *Proc. of The First International Conference on Quality of Service in Heterogeneous Wired/Wireless Networks (QShine'04)*, Oct. 2004.

[23] ——, "How well can the IEEE 802.11 wireless LAN support quality of service?" *IEEE Transaction on Wireless Communications*, vol. 4, pp. 3084–3094, 2005.

[24] X. Chen, H. Zhai, X. Tian, and Y. Fang, "Supporting QoS in IEEE 802.11e wireless LANs," *to appear in ACM Wireless Networks*, 2005.

[25] X. Chen, H. Zhai, and Y. Fang, "Enhancing the IEEE 802.11e in QoS support: analysis and mechanisms," in *Proc, of The Second International Conference on Quality of Service in Heterogeneous Wired/ Wireless Networks (QShine05)*, Aug. 2005.

[26] H. Zhai, J. Wang, and Y. Fang, "Providing statistical QoS guarantee for voice over ip in the IEEE 802.11 wireless LANs," *IEEE Wireless Communication Magazine (Special Issue on Voice over Wireless Local Area Network)*, 2006.

[27] *Cisco aironet 802.11a/b/g wireless LAN client adapters (CB21AG and PI21AG) installation and configuration guide*. Cisco Systems, Inc., 2004.

[28] *IEEE standard for wireless LAN medium access control (MAC) and physical layer (PHY) specifications, IEEE Std 802-11b-1999*, Sept. 1999.

[29] *IEEE standard for wireless LAN medium access control (MAC) and physical layer (PHY) specifications, IEEE Std 802-11g-2003*, June 2003.

[30] *IEEE standard for wireless LAN medium access control (MAC) and physical layer (PHY) specifications, IEEE Std 802-11a-1999*, 1999.

This full text paper was peer reviewed at the direction of IEEE Communications Society subject matter experts for publication in the Proceedings IEEE Infocom.